



Citation: S. Sharafi (2022) Predicting Iran's future agro-climate variability and coherence using zonation-based PCA. *Italian Journal of Agrometeorology* (2): 17-30. doi: 10.36253/ijam-1557

Received: January 29, 2022

Accepted: July 16, 2022

Published: January 29, 2023

Copyright: © 2022 S. Sharafi. This is an open access, peer-reviewed article published by Firenze University Press (<http://www.fupress.com/ijam>) and distributed under the terms of the Creative Commons Attribution License, which permits unrestricted use, distribution, and reproduction in any medium, provided the original author and source are credited.

Data Availability Statement: All relevant data are within the paper and its Supporting Information files.

Competing Interests: The Author(s) declare(s) no conflict of interest.

Predicting Iran's future agro-climate variability and coherence using zonation-based PCA

SAEED SHARAFI

Assistant Professor, Department of Environment Science and Engineering, Arak University, Arak, Iran

Corresponding author. E-mail: s-sharafi@araku.ac.ir

Abstract. The effects of climate changes on agroecosystems can cause relevant issues. Using principal component analysis (PCA) we determined the 67 agricultural climate indicators (ACI) at 44 of Iran's synoptic stations under current (1990-2019) and future (2025, 2050, 2075, and 2100) conditions. Based on UNESCO aridity index, the agroecological zonation (AEZ) was used to classify Iran's regions (very dry, dry, semidry and humid climates). Using the PCA method, the first 5 principal components were determined by including data sets for temperature (winter, spring, summer and autumn maximum and winter minimum temperature), precipitation (winter and summer precipitation), reference evapotranspiration (ET_{ref}), and the degree of growth days in spring and winter, which explained about 96 percent of the total variance. For each climate empirical equation for ET_{ref} was selected. In order to accurate evaluation of ET_{ref} were used The Penman-Monteith based on FAO_{56} (PM- FAO_{56}) for the very dry climate, the Hargreaves equation for the semidry climate, and the Penman 1 and 2 equations for the dry and humid climates, respectively. According to the results, the first component alone, with an eigenvalue of 41.15, explained more than 74 percent of the total variance. Based on the results of zoning by the PCA outcomes, the stations for 1990-2019 were classified into 7 zones. While 2025, 2050, 2075, and 2100 were classified in 6, 7, 6, and 5 zones, respectively. Under the future climatic conditions of the country, in terms of climatic indicators, the similarity between the stations will increase and the climatic diversity of the country will decline compared to current conditions. The results demonstrated that the PCA method would be valuable for monitoring AEZ in semidry climates at reasonably long periods.

Keywords: agro-climatic indicators, agro-ecological zonation, empirical equation, reference evapotranspiration.

INTRODUCTION

Climate change and variability affects agriculture more than any other human activity. Given the role of agriculture in food production, investigating the impacts of climate change on agriculture give some important elements to evaluate the world's future food security (Anwar et al., 2007; Chalinor et al., 2005; Choudhary et al., 2012; Torriani et al., 2007). In other words, these changes have a direct effect on agriculture and food security

(Brown & Funk, 2008; Schmidhuber & Tubiello, 2007). Therefore, this sector is the most vulnerable, especially in semi dry climates (Sharafi & Mir Karim, 2020).

The effect of fluctuation on climatic parameters on crops, variety and phenological stage. Therefore, climate change can reduce economic incomes by reducing production in the agricultural sector and thus reduces individuals' purchasing power, especially that of poor communities (Blazquez & Domenech, 2018). Solaymani (2018) confirmed the negative impact of rainfall-temperature variability on food availability and access to food due to a reduction in the supply of agricultural products, a commodity inflation pressure and a reduction in household income in Malaysia. Moreover, results suggest that the climate variability shocks lead to a reduction in the consumption and welfare of all household groups, particularly in rural areas.

On the basis of the aridity index of UNESCO, the climate of Iran is classified as dry climatic region (Sharafi & Ghaleni, 2021b), and therefore, its agriculture is highly dependent on precipitation and temperature. According to Rahim (2014) and Mohammed & Scholz (2019), the changes in precipitation patterns, directly and indirectly might reduce crop yield (Sánchez-Martín et al., 2017). Such changes exemplify just how much weather during the growing season, alongside long-term changes in climate, are having a significant impact on regional and global crop production (Newlands & Zamar, 2012). The effects of climate change on crop production are usually studied through crop physiology and ecology sciences. In a comprehensive review of the physiological mechanisms of crop response, various aspects of the impacts of climate change on these processes have been presented. More details of the responses of different species of crops as well as related physiological mechanisms can be reviewed from various resources (Nassiri et al., 2006; Kamali 2007). Although these studies are important in revealing crop growth responses to climate change, they do not provide data about the regional effects of climate change on crop production (e.g. rain-fed wheat). Therefore, another part of this study investigates the effect of climate change on crop production on a regional scale to provide complete information about the production situation, and future climate limitations and barriers to crop production. The complexity of such studies has led to far fewer scientific references than in the first group of studies (Hammer et al., 2001; Nassiri et al., 2006; Gholipour 2008; Sharafi et al., 2016).

Several researchers have evaluated the dependence of different empirical ET_{ref} equations on various meteorological parameters over different climates (Güçlü et al. 2017; Saggi and Jain 2019; Shiri et al. 2019; Ndiaye

et al. 2020; Sharafi and Mohammadi Ghaleni 2021a, b). Sharafi and Mohammadi Ghaleni (2021b) evaluated different empirical equations for ET_{ref} in different climates of Iran. Their results found that the simplest regression model (MLR) based on minimum and maximum temperature data was more precise than the empirical equations. They also recommended the solar radiation-based Irmak equation as the best substitute for the PM-FAO₅₆ model, especially in dry and semidry climates. Furthermore, accurate measurement of ET_{ref} is used as an indicator to understand the concepts of climate change. To better evaluate ET_{ref} in each climate, it is necessary to be aware of the climatic conditions, the quality of the weather data, and the related costs (Sharafi et al., 2016).

However, the study of the impacts of regional climate change on crop production is based on determining ACIs in the current situation, predicting future climatic conditions based on different scenarios by the current climate and climate change indicators, such as the GCM, calculation of ACIs under the conditions of climate change, comparison with the current conditions, and finally evaluation of future climatic conditions for plant growth and production (Antle, 1996; Holden & Breerton, 2004), but, the results of studies have confirmed that the PCA is suitable for analysis of agricultural climatic indicators on the regional scale and classification of stations studied in terms of similar agro-climatic characteristics (Gholipour, 2009; Nassiri & Koocheki, 2006). PCA is a statistical method that converts a set of interdependent variables into a set of independent (non-interdependent) variables (Johnson, 1998). Many researchers have used this method to homogenize interdependent climate variables and use them in subsequent statistical analysis (Briggs & Lemm, 1992; Fovell and Fovell, 1993). PCA can also establish a functional relationship between variables and a close relationship between the Pearson correlation coefficient of determination and graphical data distribution (Chatterchi & Hadi, 2012). The aim of this study is to develop and introduce ACIs by PCA on a regional scale and station zoning under future climatic conditions in very dry, dry, semi dry and humid climates. In the development of these indicators, criteria such as the availability of the required climatic parameters at the regional level and a simple and accurate working method have been considered. The introduced indicators can be calculated and applied for future time series with observational numerical values for climatic parameters under future climatic conditions (2025, 2050, 2075 and 2100) of Iran.

MATERIAL AND METHODS

Study area

Iran located in geographical coordinates between 25° and 39° north latitudes and 44° and 63° east longitudes, with an area of about 1.65×10^6 km². The long-term monthly climatic data of precipitation (mm), temperature (maximum and minimum), relative humidity, wind speed, sunshine duration, and solar radiation from 1990 up to 2019 in 44 synoptic stations have been used in this study. Data have been sourced from the Iranian Meteorological Organization of Iran (IRIMO). Some records of data input were incomplete, or not available for some stations, therefore only stations with long climatic period length remained. Due to the widespread geographical distribution of selected stations, complete coverage for different Iranian climatic regions is given. The studied synoptic stations were divided into four climatic regions, namely, very dry (13 stations), dry (15 stations), semi dry (11 stations), and humid climates (5 stations) (Table 1).

ET_{ref} evaluation

The methods for calculating ET_{ref} according to the type of input data (temperature, relative humidity, wind speed, precipitation, geographical coordinates, and altitude of each station) include seven hybrid methods based on Penman (1948), two temperature-based methods, three hybrid radiation-temperature-based methods, and a radiation-based method (Zare et al., 2006; Sharafi and Ghalenee, 2021b).

According to Sharafi and Ghaleni's (2021a) results, the ET_{ref} were estimated by empirical equations of the PM-FAO₅₆ for very dry climate, the Hargreaves equation for the semidry climate, and the Penman 1 and 2 equations for the dry and humid climates, respectively (Table 1). At the same time, the Penman-Monteith method is a suitable method in most parts of the country due to its comprehensiveness (Sharafi and Ghalenee, 2021b). This method has been used in studies by Sun and Song (2008), Gong et al. (2008), Celestin et al. (2020), and others. Since the condition for using this estimator is the normality of the studied variable (ET_{ref}), the Kolmogorov-Smirnov test was used. To evaluate the accuracy and measurement of the obtained results, there are similar statistics for measuring the validity of the models, among which is the coefficient of determination (R²), the root of square errors (RMSE), and mean bias error (MBE) (Jacovides, 1998). Based on the mentioned statistics, the most appropriate method was proposed for each climate and was considered as the basic method for the studied stations (Table 1).

The slope of the line and the coefficient of determination of ET_{ref} values (mm y⁻¹) in the 5 climates are: very dry (19.91, R² = 0.6); dry (-18.43, r = 0.72); semi dry (17.54, R² = 0.83); semi humid (9.34, R² = 0.87); and humid (57.3, R² = 0.91). The stations were divided according to ET_{ref} values. In 2019, the maximum value of ET_{ref} was detected in Chabahar (14.56 mm d⁻¹) and Abadan (13.38 mm per day); and the lowest value of ET_{ref} was at the Bandar Anzali (2.08 mm d⁻¹) and Rasht stations (2.67 mm d⁻¹), respectively.

Table 1. The values of estimated error of ET_{ref} in models used for Iran's climate.

Code	Abs.	Climate	R ²	RMSE (mm day ⁻¹)	MBE (mm day ⁻¹)	Suggested model	Reference																																	
(1)	P-M _{FAO56}	Very dry	0.92	1.33	-0.37	$ET_{ref} = \frac{0.48(R_n - G)\gamma \frac{900}{T + 273} U_2 (e_{sa} - e_a)}{\Delta + \gamma(1 + 0.34U_2)}$	Allen et al. (2006)																																	
			0.29	2.12	-0.86			(2)	P-M1	Dry	0.43	0.73	-0.24	$ET_{ref} = (2.625 + 0.000479U_2)(e_{sa} - e_a)$	Penman (1948)	0.97	1.62	-0.77	(3)	H-G	Semidry	0.77	0.88	0.15	$ET_{ref} = 0.0162(K_r, R_a, TD)^{0.5}(T + 17.8)$	Hargreaves (1975)	(4)	P-M2	Humid	0.68	0.68	0.03	$ET_{ref} = [\frac{\Delta}{\Delta + \gamma} R_n (0.27)(1 + 0.01U_2)(e_{sa} - e_a)]$	Penman (1948)	0.9	0.387	0.08	Average		
(2)	P-M1	Dry	0.43	0.73	-0.24	$ET_{ref} = (2.625 + 0.000479U_2)(e_{sa} - e_a)$	Penman (1948)																																	
			0.97	1.62	-0.77			(3)	H-G	Semidry	0.77	0.88	0.15	$ET_{ref} = 0.0162(K_r, R_a, TD)^{0.5}(T + 17.8)$	Hargreaves (1975)	(4)	P-M2	Humid	0.68	0.68	0.03	$ET_{ref} = [\frac{\Delta}{\Delta + \gamma} R_n (0.27)(1 + 0.01U_2)(e_{sa} - e_a)]$	Penman (1948)	0.9	0.387	0.08	Average			0.74	1.12	0.195								
(3)	H-G	Semidry	0.77	0.88	0.15	$ET_{ref} = 0.0162(K_r, R_a, TD)^{0.5}(T + 17.8)$	Hargreaves (1975)																																	
(4)	P-M2	Humid	0.68	0.68	0.03	$ET_{ref} = [\frac{\Delta}{\Delta + \gamma} R_n (0.27)(1 + 0.01U_2)(e_{sa} - e_a)]$	Penman (1948)																																	
			0.9	0.387	0.08			Average			0.74	1.12	0.195																											
Average			0.74	1.12	0.195																																			

ET_{ref}; reference evapotranspiration (mm day⁻¹), Δ; the slope of saturation vapor pressure curve (mb °C⁻¹), R_n; net solar radiation (MJ m⁻² day⁻¹); G; soil heat flux density (mm day⁻¹), γ; psychometric constant (kPa °C⁻¹), T_{mean}; mean daily temperature (°C), U₂; wind speed measured at 2 m height (m s⁻¹), R_a; extraterrestrial radiation (mm day⁻¹), λ; latent heat of vaporization (MJ kg⁻¹), e_{sa}; saturation vapor pressure (k Pa), e_a; actual vapor pressure (k Pa) and (e_s-e_a); saturation vapor pressure deficit (k Pa).

M-K test

Table 1 shows the seasonal climatic trends and significance at the level of 1 and 5%. According to the M-K test results, many stations show an increase in mean temperature the autumn, winter, spring and summer seasons. The slope of the warming trend was much steeper in winter and summer. In dry and very dry climates, the trend of increasing mean temperature was observed during four seasons. In general, during the last 30 years, in humid, semi dry, dry and very dry climates, about 75, 86, 81 and 89 percent of precipitation, respectively, occurs in autumn and winter, respectively. Therefore, the study of this climatic parameter has a very important role in better assessment and understanding of drought indicators. Accordingly, in all studied climates, a trend of reduced precipitation was observed, especially in winter; however, in semi dry and dry climates, this declining trend was more severe. Also, a decrease in precipitation in spring season was observed for stations in humid climate. On the other hand, in most semi dry and very dry climates, the amounts of increase in precipitation were reported in autumn season, although these values were not significant. According to the results of preliminary studies, ET_{ref} values in most of the stations studied in different climates have an increasing trend, which had an increasing and significant trend in winter and summer. The difference in ET_{ref} values in humid and very dry climates is about 2452 mm per year (Table 2).

GCM scenario

Three basic scenarios evaluate climate change impact: delta perturbation, analogue, and GCM. To a certain degree, they reflect the history of climate construction since the construction method was recognized in line with the types of available data. Delta perturbation and analogue have the simplest scenarios, whereas the GCMs are the most complex. For synthetic scenarios, a random alteration in a particular weather parameter is applied to an obtained time series. Presently, GCMs are the only reliable methods accessible for simulating the physical processes that detect the global climate situation (IPCC, 2014). Researchers depend on weather data that can be derived from GCM, which needs to be converted to a local scale using statistical or dynamical downscaling methods (Mukherjee & Siddique, 2019).

The UKMO (Version 3.0) GCM was developed at the Hadley Centre for Climate Prediction and Research, which is a part of the UK Meteorological Office. The

model is one of a breed of coupled Ocean–Atmosphere GCMs (OAGCM) that require no flux corrections to be made. The GCM consists of a linked atmospheric model, ocean model and sea ice model. However, for the present study we used only the atmospheric component of the model. By implementing UKMO-GCM for the years 2025, 2050, 2075, and 2100, the monthly values of minimum and maximum temperature, wind speed, and precipitation for different stations were calculated and the effects of climate change were determined based on the scenario defined in the model on these climatic parameters (Nassiri et al., 2006). Then, using the results of the implementation of GCM of all ACIs calculated in the current situation, again for the years 2025, 2050, 2075, and 2100, the values were calculated and by comparing these values and their differences with the current conditions, the effects of climate change on the indicators were determined (Antle, 1996).

ACI

In general, the weight of the parameters is estimated based on the relative importance of the parameters. Most of the qualitative indicators developed for the parameters used are considered unequal weights with a sum equal to one (Sarkar and Abbasi, 2006). According to an aggregation function used to calculate ACIs, the weight of each parameter has a large effect on the calculated final number (Sutadian et al., 2017; Sarkar and Abbasi, 2006; Uddin et al. 2021). In order to determine the weight for agricultural climate parameters, PCA method was used. In this method, by considering the mean values of specific vectors (α_i) related to the first 5 principal components, the weight vector related to qualitative parameters i to j (Ω_i) was calculated using Equation (5):

$$\Omega_i = \sum_{i=1}^j \lambda_i \alpha_i / P^{(j)} \quad (5)$$

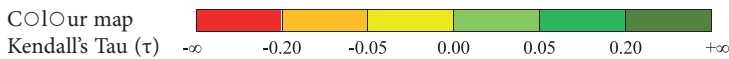
Where λ_i is the variance of the principal component of i and $P^{(j)}$ is the cumulative variance (Eq. 6) to the principal component of j .

$$P^{(j)} = \sum_{i=1}^j \lambda_i \quad (6)$$

The final weight of the parameters was calculated according to the calculated Ω_i values for each parameter i (Casillas-García et al. 2021). The aggregation of ACI is the last stage in the development of an index. In this step, using the sub-indexed parameters and the weights related to each parameter, a number was obtained as a

Tab 2. Seasonal climatic trends at the selected weather stations over Iran.

Class	Station	Tmean				Precipitation				ET _{ref}			
		Aut.	Win.	Spr.	Sum.	Aut.	Win.	Spr.	Sum.	Aut.	Win.	Spr.	Sum.
Humid	Babolsar	0.07 [△]	0.26 [▲]	0.11 [▲]	0.23 [▲]	-0.05 [▽]	-0.06	-0.07 [▽]	0.02 [●]	0.00 [●]	0.14 [▲]	0.04 [●]	0.12 [▲]
	Bandar Anzali	0.05 [●]	0.23 [▲]	0.07 [△]	0.16 [▲]	-0.05 [▽]	-0.14 [▽]	-0.07 [▽]	0.05 [△]	-0.03 [○]	0.11 [▲]	-0.01 [○]	-0.01 [○]
	Ramsar	0.07 [△]	0.27 [▲]	0.10 [△]	0.29 [▲]	0.04 [●]	0.09 [△]	-0.04 [○]	0.03 [●]	-0.01 [○]	0.16 [▲]	0.05 [●]	0.15 [▲]
	Rasht	0.07 [△]	0.20 [▲]	0.09 [△]	0.19 [▲]	-0.03 [○]	-0.04 [○]	-0.08 [▽]	0.03 [●]	-0.03 [○]	0.11 [▲]	0.02 [●]	0.04 [●]
	Gorgan	-0.05 [▽]	0.09 [△]	0.07 [△]	0.12 [▲]	-0.11 [△]	-0.09	-0.14 [△]	-0.06 [▽]	0.01 [●]	0.19 [▲]	0.15 [▲]	0.24 [▲]
Semi dry	Urmia	0.02 [●]	0.19 [▲]	0.12 [▲]	0.13 [▲]	0.02 [●]	0.02 [●]	-0.08 [▽]	0.04 [●]	0.04 [●]	0.21 [▲]	0.14 [▲]	0.18 [▲]
	Nowzheh	0.07 [△]	0.18 [▲]	0.07 [△]	0.13 [▲]	0.05 [△]	-0.18 [▽]	-0.03 [○]	0.06 [△]	0.04 [●]	0.18 [▲]	0.05 [△]	0.15 [▲]
	Sanandej	0.06 [△]	0.20 [▲]	0.13 [▲]	0.18 [▲]	0.00 [●]	-0.26 [▽]	-0.03 [○]	0.14 [▲]	0.05 [△]	0.20 [▲]	0.12 [▲]	0.23 [▲]
	Saqez	0.00 [●]	0.11 [▲]	-0.06 [▽]	-0.05 [○]	0.01 [●]	-0.15 [△]	-0.12 [△]	0.10 [△]	-0.01 [○]	0.14 [▲]	0.03 [●]	-0.01 [○]
	Arak	0.03 [●]	0.12 [▲]	0.07 [△]	0.02 [●]	-0.01 [○]	-0.22 [▽]	0.01 [●]	0.06 [△]	-0.02 [○]	0.13 [▲]	0.02 [●]	0.08 [△]
	Kermanshahan	0.09 [△]	0.17 [▲]	0.14 [▲]	0.24 [▲]	0.01 [●]	-0.11 [▽]	-0.01 [○]	0.07 [△]	0.08 [△]	0.18 [▲]	0.14 [▲]	0.28 [▲]
	Khoramabad	-0.02 [○]	0.04 [●]	0.04 [●]	0.13 [▲]	0.04 [●]	-0.12 [▽]	0.02 [●]	0.08 [△]	-0.01 [○]	0.06 [△]	0.07 [△]	0.18 [▲]
	Ilam	0.03 [●]	0.10 [△]	0.09 [△]	0.19 [▲]	0.03 [●]	-0.11 [▽]	0.01 [●]	0.08 [△]	0.03 [●]	0.12 [▲]	0.10 [△]	0.23 [▲]
	ShahreKurd	-0.06 [▽]	0.09 [△]	-0.11 [▽]	-0.16 [▽]	0.04 [●]	-0.08 [▽]	0.03 [●]	0.16 [▲]	-0.06	0.11 [▲]	-0.07 [▽]	-0.16 [▽]
	Zanjan	0.04 [●]	0.18 [▲]	0.08 [△]	0.12 [▲]	0.06 [△]	-0.05 [○]	-0.01 [○]	0.08 [△]	0.04 [●]	0.20 [▲]	0.09 [△]	0.12 [▲]
Dry	Khoy	0.07 [△]	0.15 [▲]	0.15 [▲]	0.27 [▲]	-0.03 [○]	-0.15 [▽]	-0.09 [▽]	0.10 [△]	0.07 [△]	0.16 [▲]	0.13 [▲]	0.26 [▲]
	Tabriz	0.04 [●]	0.18 [▲]	0.11 [▲]	0.17 [▲]	-0.06	-0.14 [▽]	-0.10 [▽]	0.08 [△]	0.05 [△]	0.19 [▲]	0.11 [▲]	0.18 [▲]
	Dezful	0.00 [●]	0.07 [△]	0.08 [△]	0.16 [▲]	0.03 [●]	-0.24 [▽]	-0.02 [○]	0.15 [▲]	0.19 [▲]	0.39 [▲]	0.26 [▲]	0.39 [▲]
	Birjand	0.01 [●]	0.10 [△]	0.05 [●]	0.04 [●]	0.06 [△]	-0.06 [▽]	0.05 [△]	0.10 [△]	0.01 [●]	0.12 [▲]	0.05 [●]	0.05 [●]
	Fassa	0.04 [●]	0.10 [△]	0.05 [●]	0.04 [●]	-0.01 [○]	-0.05 [○]	-0.01 [○]	0.02 [●]	-0.20 [▽]	-0.24 [▽]	-0.18 [▽]	-0.26 [▽]
	Isfahan	0.05 [●]	0.13 [▲]	0.09 [△]	0.11 [▲]	0.00 [●]	-0.05 [○]	0.04 [●]	0.02 [●]	0.05 [●]	0.14 [▲]	0.09 [△]	0.10 [△]
	Qom	0.00 [●]	0.09 [△]	0.03 [●]	0.03 [●]	0.02 [●]	-0.07 [▽]	0.04 [●]	0.06 [△]	0.01 [●]	0.11 [▲]	0.04 [●]	0.06 [△]
	Mashhad	0.12 [▲]	0.24 [▲]	0.16 [▲]	0.26 [▲]	-0.01 [○]	-0.05 [○]	0.05 [●]	0.18 [▲]	0.09 [△]	0.23 [▲]	0.14 [▲]	0.28 [▲]
	Sabzevar	0.05 [●]	0.18 [▲]	0.08 [△]	0.11 [▲]	-0.03 [○]	-0.13 [▽]	0.04 [●]	0.06 [△]	0.05 [●]	0.18 [▲]	0.08 [△]	0.13 [▲]
	Semnan	0.01 [●]	0.12 [▲]	0.09 [△]	0.09 [△]	0.03 [●]	-0.08 [▽]	0.00 [●]	0.07 [△]	-0.02 [○]	0.10 [△]	0.06 [△]	0.05 [●]
	Shahrroud	0.06 [△]	0.17 [▲]	0.11 [▲]	0.12 [▲]	-0.05 [▽]	-0.07 [▽]	-0.11 [▽]	0.11 [▲]	0.03 [●]	0.15 [▲]	0.09 [△]	0.10 [△]
	Shiraz	0.06 [△]	0.13 [▲]	0.10 [△]	0.13 [▲]	0.04 [●]	-0.06 [▽]	0.01 [●]	0.13 [▲]	0.07 [△]	0.14 [▲]	0.11 [▲]	0.16 [▲]
	Tehran	0.05 [△]	0.20 [▲]	0.10 [△]	0.13 [▲]	0.03 [●]	-0.08 [▽]	-0.02 [○]	0.13 [▲]	-0.01 [○]	0.13 [▲]	0.03 [●]	0.03 [●]
Torbate Heydarieh	0.00 [●]	0.09 [△]	0.03 [●]	0.01 [●]	0.01 [●]	-0.10 [▽]	0.02 [●]	0.10 [△]	-0.02 [○]	0.09 [△]	0.02 [●]	0.00 [●]	
Kerman	0.12 [▲]	0.17 [▲]	0.09 [△]	0.14 [▲]	0.05 [●]	-0.15 [▽]	-0.01 [○]	0.03 [●]	0.12 [▲]	0.19 [▲]	0.09 [△]	0.15 [▲]	
Very dry	Bam	0.07 [△]	0.17 [▲]	0.13 [▲]	0.21 [▲]	-0.01 [○]	-0.07 [▽]	-0.02 [○]	-0.08 [▽]	0.02 [●]	0.15 [▲]	0.10 [△]	0.21 [▲]
	Iranshahr	0.05 [●]	0.10 [△]	0.06 [△]	0.07 [△]	0.01 [●]	-0.04 [○]	0.01 [●]	0.00 [●]	0.02 [●]	0.08 [△]	0.03 [●]	0.06 [△]
	Tabass	0.11 [▲]	0.17 [▲]	0.17 [▲]	0.21 [▲]	0.02 [●]	0.04 [●]	0.01 [●]	0.04 [●]	0.11 [▲]	0.15 [▲]	0.17 [▲]	0.23 [▲]
	Yazd	0.11 [▲]	0.20 [▲]	0.12 [▲]	0.16 [▲]	0.03 [●]	-0.13 [▽]	0.04 [●]	0.15 [▲]	0.11 [▲]	0.20 [▲]	0.11 [▲]	0.18 [▲]
	Zabol	0.05 [●]	0.11 [▲]	0.10 [△]	0.19 [▲]	0.00 [●]	-0.09 [▽]	0.06 [△]	-0.06 [▽]	0.03 [●]	0.14 [▲]	0.09 [△]	0.18 [▲]
	Zahedan	0.06 [△]	0.14 [▲]	0.10 [△]	0.09 [△]	0.00 [●]	-0.05 [▽]	0.02 [●]	0.14 [▲]	0.05 [△]	0.15 [▲]	0.07 [△]	0.09 [△]
	Abadan	0.07 [△]	0.15 [▲]	0.15 [▲]	0.31 [▲]	0.01 [●]	-0.14 [▽]	0.03 [●]	-0.02 [○]	0.06 [△]	0.14 [▲]	0.16 [▲]	0.34 [▲]
	Ahwaz	0.09 [△]	0.17 [▲]	0.17 [▲]	0.27 [▲]	-0.03 [○]	-0.12 [▽]	-0.01 [○]	-0.04 [○]	-0.04 [○]	0.05 [△]	-0.02 [○]	-0.15 [▽]
	Bandar Abbas	0.03 [●]	0.08 [△]	0.03 [●]	0.02 [●]	0.10 [△]	-0.06 [▽]	0.05 [●]	0.11 [▲]	-0.28 [▽]	-0.30 [▽]	-0.31 [▽]	-0.35 [▽]
	Bandar Lengeh	0.12 [▲]	0.20 [▲]	0.12 [▲]	0.26 [▲]	0.09 [△]	-0.10 [▽]	0.03 [●]	0.02 [●]	0.05 [●]	0.13 [▲]	0.07 [△]	0.22 [▲]
	Bushehr	0.07 [△]	0.16 [▲]	-0.01 [○]	0.00 [●]	0.05 [●]	-0.08 [▽]	0.03 [●]	0.30 [▲]	0.02 [●]	0.12 [▲]	-0.17 [▽]	-0.31 [▽]
	Chabahar	0.06 [△]	0.13 [▲]	0.06 [△]	0.00 [●]	-0.02 [○]	-0.08 [▽]	-0.01 [○]	-0.05 [○]	-0.13 [▽]	-0.09 [▽]	-0.18 [▽]	-0.25 [▽]
	Jask	0.11 [▲]	0.21 [▲]	0.10 [△]	0.08 [△]	0.05 [●]	-0.14 [▽]	0.14 [▲]	-0.06 [▽]	0.17 [▲]	0.25 [▲]	0.14 [▲]	0.14 [▲]



▲, significant at 1% with increasing trend; ▼, significant at 1% with decreasing trend; △, significant at 5% with increasing trend; ▽, significant at 5% with decreasing trend; ●, not significant with increasing trend; ○, not significant with decreasing trend.

score for the quality of the parameter. The aggregation function of ACI can be additive functions, multiplicative functions or a combination of these two functions (Sutadian et al., 2016).

In order to evaluate 67 agricultural climate indicators, 36 temperature variables including; the minimum temperature in winter (12 variables), the maximum temperature in winter (12 variables), winter precipitation (6 variables), summer precipitation (6 variables), the maximum temperature in spring, summer, and autumn (12 variables), ET_{ref} (12 variables) in different seasons, degree of growth days in spring and winter (4 variables) and forest day in spring, fall and winter seasons (3 variables) (Appendix 1). The PCA technique was used to evaluate ACIs at 44 stations in Iran. SAS software (V.13.1) was used to perform PCA (Rosenzweig et al., 1995). For this purpose, 67 ASCII data files were first placed in a set. The PRIN COMP PROC command was used to provide principal components of the data. The principal components were implemented in the correlation matrix because the analyzed variables had very different numerical values and their mean and standard deviation were very different due to measurement in different units. It should be noted that the application of PCA on the coefficient of determination matrix is equivalent to the application of this technique on standardized data (Fovell & Fovell, 1993). According to the PCA results, eigenvalues and eigenvectors related to each of the principal components were calculated and evaluated (Nassiri et al., 2006). ACIs of different stations, calculated based on the results of the GCM model under climate change conditions, were also exposed to PCA after becoming 67 indicators and their principal components under climate change conditions were determined. Finally, all ACIs calculated under the current conditions and different scenarios of climate change along with their principal components were compared and the effect of climate change on these indicators was evaluated (Appendix 1).

RESULTS AND DISCUSSION

Statistical analysis of ACIs

Having implemented PCA, the first 5 principal components explained about 100 percent of the total variance. In general, statistically speaking, there is no specific method for selecting the number of components that should be retained, so selecting 5 components in this study was a judgment call. Note, however, that the simplest criterion for selecting the number of components is to retain a number that can explain 95 percent of the total variance. Accordingly, the presence of 4

principal components was sufficient to explain 95 percent of the total variance. Further analysis showed that it is not necessary to add a new component because by excluding the fifth component, the statistical accuracy of the next analysis was not much reduced. Table 2 presents the eigenvalues of the coefficient of the determination matrix and the part of the total variance explained by each of the 5 principal components. According to the results, the first component with an eigenvalue of 41.15 alone explained more than 75 percent of the total variance. These values are reduced in subsequent components, respectively, and finally the fifth component, with an eigenvalue less than one, explained a small amount of the total variance percentage. Furthermore, the first four principal components can explain 98.85 percent of the total variance; however, as mentioned earlier, the presence of the fifth component only improved the accuracy of this analysis and subsequent analysis (Table 3).

Appendix 1 presents eigenvalues for each of 67 variables in 5 principal components. As shown, the first principal component is filled with load temperature variables (variables 1 to 36 of Appendix 1). Load or loading is the power (with values from -1 to +1) of the coefficients related to each of the variables integrated into a principal component. The highest load of the second principal component is related to the winter minimum temperature, the winter precipitation, and the variables of autumn, winter and spring precipitation and ET_{ref} (variables 4, 12, and 37-60 of Appendix 1). The maximum load of the third principal component is the winter minimum, average, and maximum temperature (variables 16, 20, and 24 of Appendix 1). The fourth principal component showed its highest load for the summer minimum, average, and maximum temperature, the spring maximum temperature, and the winter minimum, average, and maximum precipitation and ET_{ref}

Table 3. Eigenvalues of the correlation matrix and amount of variance described by each of the 5 principal components.

PCA	Eigenvalue	Difference*	Ratio of total variance	Cumulative ratio of total variance**
PCA 1	0.7689	0.7358	32.0756	40.8927
PCA 2	0.9265	0.1563	6.2138	9.3025
PCA 3	0.9734	0.0542	2.0022	3.0531
PCA 4	0.9814	0.0191	0.2093	1.0526
PCA 5	0.9991	0.0148	0.1208	0.8409

* The difference between the eigenvalues of two successive components.

** The cumulative value of the ratio of variance described by successive components.

Table 4. The description of information for each of the 5 principal components.

PCA	Description information
PCA 1	The sum information of temperature (min, max, and mean)
PCA 2	The winter minimum temperature and ET_{ref}
PCA 3	The winter minimum and average ET_{ref} , the winter minimum temperature
PCA 4	The winter precipitation, the summer ET_{ref} , the spring, summer, and autumn maximum temperature
PCA 5	Growth degree days (GDD) in spring and winter, the summer precipitation

(variables 17, 18, 22, 17, 17, 40, 44, 48, 52, 56 and 60 in Appendix 1). The fifth principal component had a positive load for variable degree of growth days in winter and spring, and the spring minimum, maximum, and average precipitation (variables 32, 38, 39, 42, 46, 50, 54, and 58 of Appendix 1). Accordingly, Table 4 summarizes the information integrated into each of the 5 principal components, which together explain 99 percent of the total variance in agricultural climate data.

In this study, using the geographic information system related to the country's stations, after implementation of the program and based on the variables integrated into the 5 principal components, the stations were placed in seven climatic areas. Fig. 2 shows the location of these areas based on the first and second principal components, which together explain about 91 percent of the total variance among the data (Table 3). Therefore, according to the set of indicators of agricultural climatology used in this study, stations with the maximum climatic similarity were placed in a group. It is not possible to group the studied stations based on 67 indicators at a stage. Therefore, as mentioned earlier, at the first stage the indicators of agricultural climatology were placed in 5 principal components, and then, by the geographic information system based on the principal components, the stations of the same climate were placed in the same area.

Statistical analysis of agricultural climatic indices under conditions of climate change

The results of statistical analysis showed that under the conditions of climate change, 4 principal components will explain more than 96 percent of the total data variance, while in the current situation, to explain the variance of agricultural climate data, 5 principal components were defined (Table 3). The properties of the 4 components related to climate change conditions are

Table 5. The description of information for each of the 5 principal components of climate change (2025, 2050, 2075, and 2100).

PCA	Description information
PCA 1	The summed information of temperature (min, max, and mean, respectively)
PCA 2	ET_{ref}
PCA 3	The autumn minimum temperature, the summer maximum temperature
PCA 4	The winter ET_{ref} , growing degree days in spring

presented in Table 5. Also, the first and the second, are the same in the current situation and under climate change conditions, but the other components are different (Table 5). Various researchers have cited temperature, precipitation, and the climatic indicators of their crops (e.g. the duration of the growing season or of the dry season) as the most important variables affecting crop growth and development.

The results show that under climate change conditions, the set of information about temperature, precipitation, and the indicators obtained from them will be the principal climatic components in Iran; however, the contribution of these components to explaining the properties of the studied stations compared with different current conditions is somehow different. These results are consistent with the study results of Solaymani et al. (2018), who examined the effects of climate change on Malaysian food security. Table 6 presents the eigenvalues and the amount of variance explained by each of the principal components under climate change conditions. Comparing these results with the values presented in Table 6 shows that under climate change conditions, the contribution of the first principal component (temperature information) to the explanation of total has declined and in contrast, the role of the second principal component (precipitation information) in overall variance has increased; in addition, the second principal component for 2050 has been much more effective than 2025 and 2100. In other words, the second principal component will have a decreasing trend of precipitation and an increasing trend of temperature. Therefore, it seems that under future climate change conditions of the country, the amount of precipitation and agricultural climate indicators related to it will be more important compared to the current situation, and in contrast to the role of temperature and its indicators, will be somewhat reduced compared to specific conditions. Accordingly, it can be concluded that although the increase in temperature in many parts of the country will prolong the growing season, at the same time an increase in the

Table 6. The eigenvalues and described variance for each of the 5 principal components in the situation of climate change (2025, 2050, 2075, and 2100) based on the results of the general circulation model (GCM).

PCA	Eigenvalues				Ratio of total variance				Cumulative ratio of total variance*			
	2025	2050	2075	2100	2025	2050	2075	2100	2025	2050	2075	2100
PCA 1	0.49207	0.50396	0.54910	0.60579	0.49207	0.50396	0.54910	0.60579	25.8314	27.1001	31.020	37.1914
PCA 2	0.94048	0.87647	0.89778	0.89174	0.44841	0.37251	0.34868	0.28595	24.1833	22.1990	20.1212	17.3120
PCA 3	0.96177	0.90782	0.94274	0.94443	0.02129	0.03135	0.04496	0.05269	2.8616	2.0312	2.4511	3.0824
PCA 4	0.97871	0.92186	0.95802	0.95998	0.01694	0.01404	0.01528	0.01555	1.0281	0.8817	0.9142	0.9101

* The cumulative value of the ratio of variance described by successive components.

duration of the dry season will create limitations for new agricultural climate indicators that are not very obvious in the current situation. Confirmation of this conclusion requires further studies on the growth and development responses of crops under the expected future climatic conditions of Iran.

Fig. 1 shows the zoning of stations by PCA in terms of agricultural climate indicators (1990-2019). Based on this, the studied stations are located in 6 classes but the second class was not located in any of the climatic zones. The northern regions of the country were located in class 7 and the southern, southwestern, and southeastern regions were located in class 1. There is climatic diversity in the western and northwestern regions of the country. By crossing the northwest and west of the country to the central, southern, northern, and eastern regions, climate diversity is reduced and the country is divided into two parts including humid (class 7) and very dry (south, center, and east) climates. The southern coastal region, due to rising temperatures and lack of suitable vegetation, and despite its high relative humidity, was located in class 1 (Table 7).

Agricultural climate data for the studied stations were reclassified after determining the PCA under climate change conditions. The position of the stations under climate change conditions is shown in Fig. 2 for the years 2025 (6 zones), 2050 (7 zones), 2075 (6 zones), and 2100 (5 zones) (Table 8). According to these results, under future climatic conditions of the country, the similarity between the climates will increase in terms of ACIs, and in fact, the climatic diversity of the country's agriculture will decline compared to current conditions. Also, with the intensification of future climate change, as shown in Fig. 2, the density of stations within each area increase, confirming the uniformity of conditions in that climate.

Although the effect of climate change on Iran's climate is not certain, the study results of various researchers confirm this (Nassiri et al., 2006). On the one hand, the effect of climate change on agricultural climatic

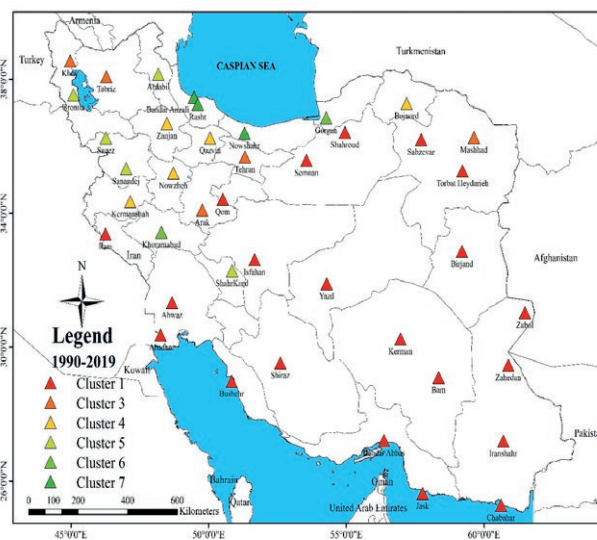


Fig. 1. Map showing the zoning of stations based on PCA (1990-2019).

indicators and finally the displacement of agricultural climatic areas has been reported by some researchers (Antle, 1996; Rosenzweig et al., 1995). For example, Holden and Brereton (2004) and Araya et al. (2010) showed that future climate change would affect agricul-

Table 7. The classification of stations based on PCA (1990-2019).

Class	Stations
1	Abadan, Ahwaz, Bam, Birjand, Bandar Abbas, Bushehr, Chabahar, Ilam, Jask, Qom, Kerman, Sabzevar, Semnan, Shahroud, Shiraz, Tehran, Torbat Heydarieh, Yazd, Zabol, Zahedan, Iranshahr, Isfahan
3	Arak, Khoy, Mashhad, Tabriz
4	Bojnord, Nozheh, Kermanshah, Qazvin, Zanjan
5	Ardabil, Urmia, Saqez, Sanandej, ShahreKurd
6	Gorgan, Khoramabad
7	Bandar Anzali, Rasht, Nowshahr

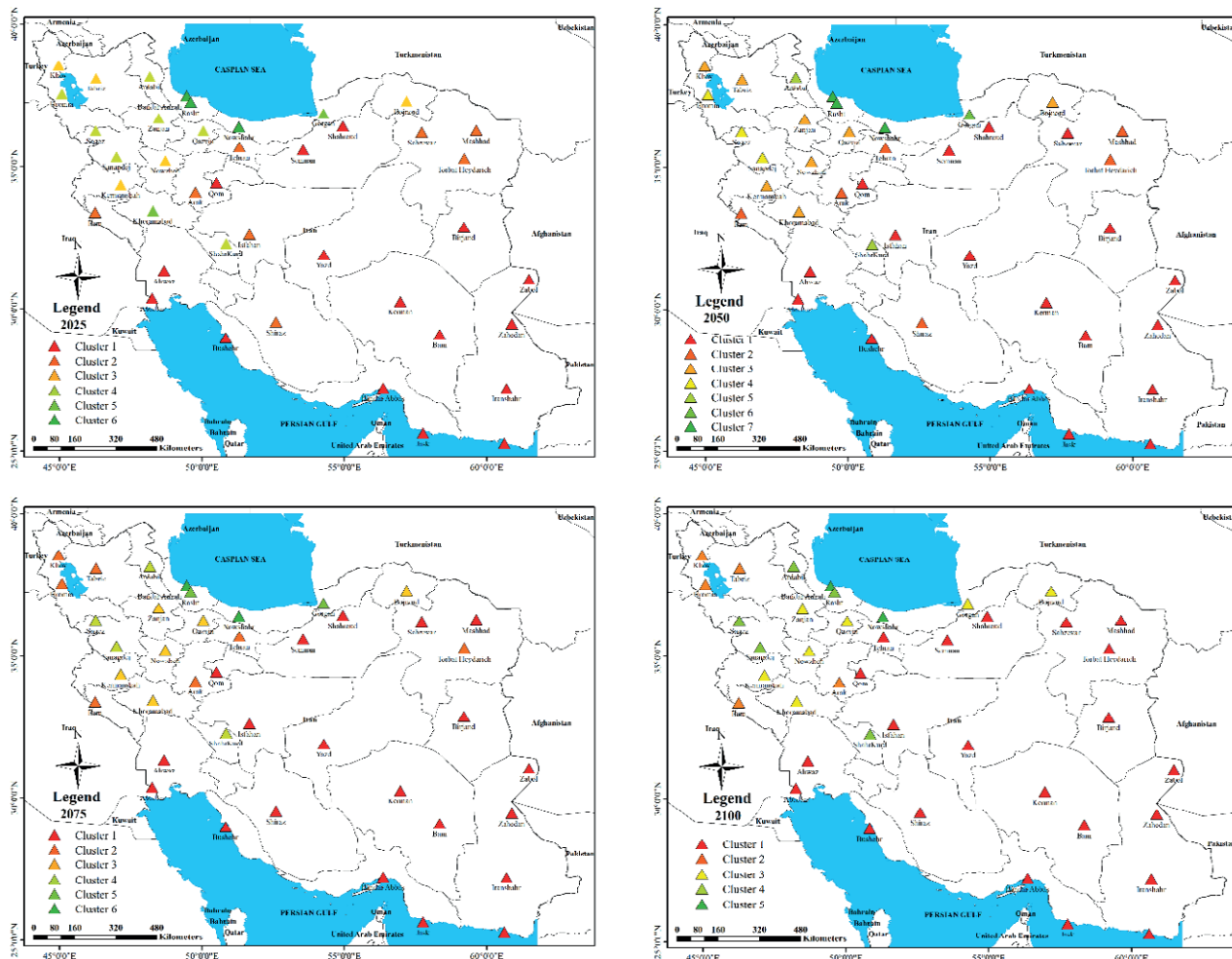


Fig. 2. The predicted maps of climate classification based on PCA for 2025, 2050, 2075, and 2100 in Iran.

tural climate climates, reducing potential crop production in Ireland and Ethiopia, respectively. Solymani (2018) also showed that climate variables reduce the food security and well-being of poor families, especially in rural areas of Malaysia. Accordingly, and considering the results obtained in the case of Iran, it seems that the effects of climate change on a regional scale along with studies on the physiological consequences of this phenomenon are important and should be considered.

Vaghefi et al. (2019) used five climate models to project temperature and precipitation distribution across Iran. They confirmed that compared to the period of 1980–2004, in the period of 2025–2049, Iran is likely to experience more extended periods of extreme temperatures in the dry and very dry climates (for ≥ 120 days: precipitation < 2 mm, $T_{max} \geq 30^\circ C$) as well as humid climates (for ≤ 3 days: total precipitation ≥ 110 mm) conditions. Also, Panahi et al. (2020) evaluated data time

series of temperature, precipitation, runoff, ET_{ref} and water storage change, to determine their situation and variations in Iran (1986–2016). They found that the country warmed, precipitation typically decreased, while ET_{ref} increased in dry and very dry climates. Overall, the extra water provided from primarily groundwater depletion has fed and kept ET_{ref} at levels beyond those sustained by the annually renewable water input from precipitation. Therefore, this shows unsustainable water consumption for maintaining and expanding human activities, such as irrigated agriculture.

CONCLUSIONS

The study results show that the PCA method under climate change conditions explained more than 96 percent of the observed changes among the climatic data

Table 8. The predicated stations classification based on PCA for 2025, 2050, 2075 and 2100 in Iran.

Year	Class	Stations
2025		Abadan, Ahwaz, Bam, Birjand, Bandar Abbas, Bushehr, Chabahar, Jask, Qom, Kerman, Semnan, Shahroud, Yazd, Zabol, Zahedan, Iranshahr
	1	
	2	Arak, Mashhad, Sabzevar, Shiraz, Tehran, Torbat Heydarieh, Ilam, Isfahan
	3	Bojnord, Khoy, Nozheh, Kermanshah, Tabriz
	4	Ardabil, Qazvin, Urmia, Saqez, Sanandej, ShahreKurd, Zanjan
	5	Gorgan, Khoramabad
2050	6	Bandar Anzali, Rasht, Nowshahr
		Abadan, Ahwaz, Bam, Birjand, Bandar Abbas, Bushehr, Chabahar, Jask, Qom, Kerman, Sabzevar, Semnan, Shahroud, Yazd, Zabol, Zahedan, Iranshahr, Isfahan
	1	
	2	Arak, Mashhad, Shiraz, Tehran, Torbat Heydarieh, Ilam
	3	Bojnord, Qazvin, Nozheh, Khoramabad, Kermanshah, Khoy
	4	Urmia, Saqez, Sanandej
	5	Ardabil, ShahreKurd
6	Gorgan	
2075	7	Bandar Anzali, Rasht, Nowshahr
		Abadan, Ahwaz, Bam, Birjand, Bandar Abbas, Bushehr, Chabahar, Jask, Qom, Kerman, Sabzevar, Semnan, Shahroud, Yazd, Zabol, Zahedan, Iranshahr, Isfahan, Mashhad, Shiraz
	1	
	2	Arak, Khoy, Urmia, Tabriz, Tehran, Torbat Heydarieh, Ilam
	3	Bojnord, Qazvin, Nozheh, Khoramabad, Kermanshah, Zanjan
	4	Ardabil, ShahreKurd, Saqez, Sanandej
2100	5	Gorgan, Rasht
	6	Bandar Anzali, Nowshahr
		Abadan, Ahwaz, Bam, Birjand, Bandar Abbas, Bushehr, Chabahar, Jask, Qom, Kerman, Sabzevar, Semnan, Shahroud, Yazd, Zabol, Zahedan, Iranshahr, Isfahan, Mashhad, Shiraz, Tehran, Torbat Heydarieh
	1	
	2	Arak, Khoy, Urmia, Tabriz, Ilam
	3	Bojnord, Qazvin, Nozheh, Khoramabad, Kermanshah, Zanjan, Gorgan
	4	Ardabil, ShahreKurd, Saqez, Sanandej, Rasht
	5	Bandar Anzali, Nowshahr

of the 44 weather nation-wide stations studied. Note that the first two principal components, i.e. temperature and precipitation information and their associated climatic indicators (especially ET_{ref} which is a combination of all climatic parameters) explained more than 90 percent of the change in the current situation and climate change. However, if future changes occur, the contribution of precipitation to the current situation will increase and the role of the temperature will reduce relatively. According to the results, it seems that under these conditions, Iran's climatic diversity has already been reduced to some extent and the climatic similarity between the areas is increasing. Therefore, given the climatic stability of the country's very dry climates till 2050 and the addition of stations located in dry climate to a very dry climate by 2100, the central, western, and northwestern, eastern, and southeastern regions are expected to be under very dry conditions.

It is necessary to mention that each developed index has advantages and disadvantages and can be used in a

limited situation and for specific purposes. High uncertainty, specific and limited application, and overestimation or underestimation are among the most important disadvantages of most agro-climatological indicators. Therefore, confirmation of these results requires more extensive studies (review of more diverse models), especially the growth response of plants in the future climatic conditions of Iran. Given that only one general circulation model was used in the present study, it is suggested that more models be used in future research.

REFERENCES

- Allen R.G., Pruitt W.O., Wright J.L., Howell T.A., Ventura F., Snyder R., ... & Elliott R., 2006. A recommendation on standardized surface resistance for hourly calculation of reference ETo by the FAO56 Penman-Monteith method, *Agricultural Water Management*, 81(1-2), 1-22.

- Antle J.M., 1996. Methodological issues in assessing potential impacts of climate change on agriculture, *Agricultural and Forest Meteorology*, 80(1), 67-85.
- Anwar M.R., O'Leary G., McNeil D., Hossain H., Nelson R., 2007. Climate change impact on rainfed wheat in south-eastern Australia, *Field crops research*, 104(1-3), 139-147.
- Araya A., Keesstra S.D., Stroosnijder L., 2010. A new agro-climatic classification for crop suitability zoning in northern semi-arid Ethiopia, *Agricultural and forest meteorology*, 150(7-8), 1057-1064.
- Blazquez D., Domenech J., 2018. Big Data sources and methods for social and economic analyses, *Technological Forecasting and Social Change*, 130, 99-113.
- Briggs R.D., Lemin J.R.C., 1992. Delineation of climatic regions in Maine, *Canadian Journal of Forest Research*, 22(6), 801-811.
- Brown M.E., Funk C.C., 2008. Food security under climate change.
- Casillas-García L.F., de Anda, J., Yebra-Montes, C., Shear, H., Díaz-Vázquez, D., Gradilla-Hernández, M.S., 2021. Development of a specific water quality index for the protection of aquatic life of a highly polluted urban river, *Ecological Indicators*, 129, 107899.
- Celestin S., Qi F., Li R., Yu T., Cheng W., 2020. Evaluation of 32 simple equations against the Penman-Monteith method to estimate the reference evapotranspiration in the Hexi corridor, *Northwest China. Water*, 12(10), 2772.
- Challinor A.J., Wheeler T.R., Craufurd P.Q., Slingo J.M., 2005. Simulation of the impact of high temperature stress on annual crop yields, *Agricultural and Forest Meteorology*, 135(1-4), 180-189.
- Choudhary J.S., Shukla G., Prabhakar C., Maurya S., Das B., Kumar S., 2012. Assessment of local perceptions on climate change and coping strategies in Chotanagpur Plateau of Eastern, *India Journal of Progressive Agriculture*, 3, 8-15.
- Doorenbos J., Pruitt W.O., 1977. Guidelines for predicting crop water requirements, Irrigation and drainage paper No 24, 2nd edn, Food and Agriculture Organization, Rome, p 156.
- Fovell R.G., Fovell M.-Y.C. (1993) Climate zones of the conterminous United States defined using cluster analysis. *Journal of Climate* 6: 2103-2135
- Hargreaves G.H., 1975. Moisture availability and crop production, *Transactions of the ASAE*, 18(5), 980-984.
- Gholipoor M., 2009. Evaluating the effect of crop residue on water relations of rainfed chickpea Maragheh, Iran, using simulation.
- Gholipoor M., 2008. Quantifying the threshold frost hardness for over-wintering survival of wheat in Iran, using simulation. *International J. Plant Production*, 2(2), 125-136.
- Gong L., Xu C.Y., Chen D., Halldin S., Chen Y.D., 2006. Sensitivity of the Penman-Monteith reference evapotranspiration to key climatic variables in the Changjiang (Yangtze River) basin, *Journal of hydrology*, 329(3-4), 620-629.
- Güçlü Y.S., Subyani A.M., Şen Z., 2017. Regional fuzzy chain model for evapotranspiration estimation, *Journal of hydrology*, 544, 233-241.
- Hammer G.L., Hansen J.W., Phillips J.G., Mjelde J.W., Hill H., Love A., Potgieter, A., 2001. Advances in application of climate prediction in agriculture, *Agricultural systems*, 70(2-3), 515-553.
- Holden N.M., Brereton A.J., 2004. Definition of agroclimatic regions in Ireland using hydro-thermal and crop yield data, *Agricultural and Forest Meteorology*, 122(3-4), 175-191.
- IPCC., 2014. Intergovernmental Panel on Climate Change. Climate Change 2014: impacts, adaptation, and vulnerability <http://www.ipcc.ch/report/ar5/wg2>. Accessed 15 May 2015
- Jacovides C.P., 1998. Reply to comment on "Statistical procedures for the evaluation of evapotranspiration computing models", *Agricultural water management*, 37(1), 95-97.
- Johnson D.E., 1998. Applied multivariate methods for data analysts, Duxbury Resource Center.
- Kamali M.R., 2007. World situation of Wheat in the past, present, and future. 10th congress of agronomy and modification of plants, Karaj, Iran. 23-45.
- Mohammed R., Scholz M., 2019. Climate variability impact on the spatiotemporal characteristics of drought and Aridity in arid and semi-arid regions, *Water Resources Management*, 33(15), 5015-5033.
- Mukherjee N., Siddique G., 2019. Assessment of climatic variability risks with application of livelihood vulnerability indices, *Environment, Development and Sustainability*, 1-27.
- Nassiri M., Koocheki A., Kamali G.A., Shahandeh H., 2006. Potential impact of climate change on rainfed wheat production in Iran: (Potentieller Einfluss des Klimawandels auf die Weizenproduktion unter Rainfed-Bedingungen im Iran), *Archives of agronomy and soil science*, 52(1), 113-124.
- Newlands N.K., Zamar, D.S., 2012. In-season probabilistic crop yield forecasting, integrating agro-climate, remote-sensing and phenology data.
- Ndiaye P.M., Bodian A., Diop L., Deme A., Dezetter A., Djaman K., 2020. Evaluation and Calibration of Alternative Methods for Estimating Reference Evapotranspiration in the Senegal River Basin, *Hydrology*, 7, 24.

- Panahi D.M., Kalantari Z., Ghajarnia N., Seifollahi-Aghmiuni S., Destouni G., 2020. Variability and change in the hydro-climate and water resources of Iran over a recent 30-year period. *Scientific reports*, 10(1), 1-9.
- Penman H.L., 1948. Natural evaporation from open water, bare soil and grass. Proceedings of the Royal Society of London, Series A. *Mathematical and Physical Sciences*, 193(1032), 120-145.
- Rahim S.A., 2014. VIA of climate change on Malaysian agriculture systems: Current understanding and plans. University Kebangsaan Malaysia, http://www.ukm.my/seaclidcordex/presentation_rice_project.html.
- Rosenzweig C., Ritchie J.T., Jones J.W., Tsuji G.Y., Hildebrand P., 1995. Climate change and agriculture: analysis of potential international impacts. In Symposium on Climate Change and Agriculture: Analysis of Potential International Impacts (No. RESEARCH). Soil Science Society of America.
- Saggi M.K., Jain S., 2019. Reference evapotranspiration estimation and modeling of the Punjab Northern India using deep learning, *Computers and Electronics in Agriculture*, 156, 387-398.
- Sánchez-Martín, J., Rispail, N., Flores, F., Emeran, A. A., Sillero, J. C., Rubiales, D., Prats, E., 2017. Higher rust resistance and similar yield of oat landraces versus cultivars under high temperature and drought. *Agronomy for sustainable Development*, 37(1), 1-14.
- Sarkar C., Abbasi, S.A., 2006. QUALIDEX—a new software for generating water quality indices, *Environmental monitoring and assessment*, 119(1), 201-231.
- Schmidhuber J., Tubiello, F.N., 2007. Global food security under climate change, *Proceedings of the National Academy of Sciences*, 104(50), 19703-19708.
- Sharafi S., Ghaleni M.M., 2021a. Calibration of empirical equations for estimating reference evapotranspiration in different climates of Iran, *Theoretical and Applied Climatology*, 1-15.
- Sharafi S., Ghaleni, M.M., 2021b. Evaluation of multivariate linear regression for reference evapotranspiration modeling in different climates of Iran, *Theoretical and Applied Climatology*, 143(3), 1409-1423.
- Sharafi S., Karim N.M., 2020. Investigating trend changes of annual mean temperature and precipitation in Iran, *Arabian Journal of Geosciences*, 13(16), 1-11.
- Sharafi S., Ramroudi M., Nasiri M., Galavi M., Kamali G.A., 2016. Role of early warning systems for sustainable agriculture in Iran, *Arabian Journal of Geosciences*, 9(19), 1-17.
- Shiri J., Marti P., Karimi S., Landeras G., 2019. Data splitting strategies for improving data driven models for reference evapotranspiration estimation among similar stations, *Computers and Electronics in Agriculture*, 162, 70-81.
- Solaymani S., 2018. Impacts of climate change on food security and agriculture sector in Malaysia, *Environment, Development and Sustainability*, 20(4), 1575-1596.
- Sun L., Song C., 2008. Evapotranspiration from a freshwater marsh in the Sanjiang Plain, Northeast China, *Journal of Hydrology*, 352(1-2), 202-210.
- Sutadian A.D., Muttill, N., Yilmaz, A.G., Perera, B.J.C., 2017. Using the Analytic Hierarchy Process to identify parameter weights for developing a water quality index, *Ecological Indicators*, 75, 220-233.
- Torriani D.S., Calanca P., Schmid S., Beniston M., Fuhrer J., 2007. Potential effects of changes in mean climate and climate variability on the yield of winter and spring crops in Switzerland, *Climate Research*, 34(1), 59-69.
- Uddin M.G., Nash, S., Agnieszka, I., 2021. A review of water quality index models and their use for assessing surface water quality. In *Ecological Indicators*, 122, p. 107218. DOI: 10.1016/j.ecolind.2020.107218.
- Vaghefi S.A., Keykhai M., Jahanbakhshi F., Sheikholeslami J., Ahmadi A., Yang H., Abbaspour K.C., 2019. The future of extreme climate in Iran. *Scientific reports*, 9(1), 1-11.
- Zare Feyz Abadi A., Koochaki A., Nassiri Mahalati M., 2006. Trend analysis of yield, production and cultivated area of cereal in Iran during the last 50 years and prediction of future situation, *Iranian Journal of Field Crops Research*, 4(1), 49-70.

Appendix 1. The special vectors of the main components.

Variable	Variable description	PC 1	PCA 2	PCA 3	PCA 4	PCA 5
Temperature						
VAR1	tmin_minsp	0.16450	0.14441	0.02848	-0.12959	-0.00295
VAR2	tmin_minsu	0.12960	0.05561	0.00245	0.08367	0.04738
VAR3	tmin_minf	0.14060	0.12796	-0.03723	-0.04595	-0.02857
VAR4	tmin_minw	0.11160	0.21297	0.04838	-0.22508	-0.09398
VAR5	tmin_maxsp	0.15854	0.09397	-0.21826	-0.18485	0.00927
VAR6	tmin_maxsu	0.13953	0.02859	-0.22820	-0.00255	0.04716
VAR7	tmin_maxf	0.11035	0.09375	-0.21926	-0.16883	0.01272
VAR8	tmin_maxw	0.13504	0.15051	0.03738	-0.23938	-0.03640
VAR9	tmin_avgsp	0.13949	0.12921	-0.12072	0.00945	-0.00616
VAR10	tmin_avgsu	0.16554	0.02086	-0.26172	-0.01299	0.02835
VAR11	tmin_avgf	0.12383	0.11950	-0.13281	-0.16266	-0.01949
VAR12	tmin_avgw	0.10964	0.22985	0.00949	-0.14321	0.00272
VAR13	tmax_minsp	0.11360	0.01850	0.12050	0.07398	0.00650
VAR14	tmax_minsu	0.16348	-0.05825	0.03838	0.21946	0.09288
VAR15	tmax_minf	0.15027	-0.06380	0.12942	0.08409	-0.01628
VAR16	tmax_minw	0.12897	0.04636	0.21245	-0.07848	-0.03858
VAR17	tmax_maxsp	0.17035	-0.03850	0.03988	0.19298	0.01848
VAR18	tmax_maxsu	0.14478	-0.13740	0.00949	0.20209	0.01949
VAR19	tmax_maxf	0.13894	-0.08450	0.04848	0.18939	0.01849
VAR20	tmax_maxw	0.13034	0.04738	0.31949	-0.01748	-0.00140
VAR21	tmax_avgsp	0.18043	0.00187	0.09844	0.13938	0.02385
VAR22	tmax_avgsu	0.13222	-0.08056	0.02848	0.21041	0.01295
VAR23	tmax_avgf	0.14006	-0.07521	0.09387	0.13939	-0.03925
VAR24	tmax_avgw	0.14039	0.02815	0.34939	-0.02646	-0.04848
VAR25	tavg_minsp	0.14887	0.08386	0.06851	-0.01285	-0.00464
VAR26	tavg_minsu	0.16941	-0.00221	-0.06816	0.12948	0.04839
VAR27	tavg_minf	0.18247	0.04840	0.08738	0.09359	-0.04921
VAR28	tavg_minw	0.11841	0.12960	0.20195	-0.20849	-0.04849
VAR29	tavg_maxsp	0.14847	0.00066	-0.06386	0.12249	0.02858
VAR30	tavg_maxsu	0.11048	-0.04816	-0.11027	0.12939	0.02859
VAR31	tavg_maxf	0.14354	0.08285	-0.07382	0.07377	0.02858
VAR32	tavg_maxw	0.11588	0.11941	0.19384	-0.13939	-0.04849
VAR33	tavg_avgsp	0.13570	0.04840	-0.05463	0.02783	0.02858
VAR34	tavg_avgsu	0.14942	0.02046	-0.02027	0.11409	0.02906
VAR35	tavg_avgf	0.16247	0.01295	-0.00112	0.01946	-0.00927
VAR36	tavg_avgw	0.12360	0.11951	0.11782	-0.09387	-0.10395
Precipitation						
VAR37	ppt_minsp	-0.08707	0.26999	0.04887	0.14991	0.03001
VAR38	ppt_minsu	-0.11046	0.13127	-0.03981	-0.06542	0.26653
VAR39	ppt_minf	-0.103	0.25092	0.02090	0.12942	0.00538
VAR40	ppt_minw	-0.09034	0.25978	-0.01092	0.27551	-0.04027
VAR41	ppt_maxsp	-0.12041	0.24091	0.02219	0.13090	0.03639
VAR42	ppt_maxsu	-0.13914	0.16592	0.06048	-0.00776	0.19442
VAR43	ppt_maxf	-0.07797	0.22092	-0.00337	0.22082	-0.00548
VAR44	ppt_maxw	-0.07806	0.26507	0.01093	0.25047	-0.06542
VAR45	ppt_avgsp	-0.12313	0.25082	0.03129	0.13092	0.00438
VAR46	ppt_avgsu	-0.13423	0.12002	-0.00897	0.06199	0.23693
VAR47	ppt_avgf	-0.01865	0.27227	-0.00598	0.12783	-0.00819
VAR48	ppt_avgw	-0.09995	0.25548	0.00167	0.25582	-0.09694

			ET _{ref}			
VAR49	eto-minsp	-0.01805	0.24907	0.03588	0.11597	0.03247
VAR50	eto-minsu	-0.14730	0.11586	-0.06691	0.25955	0.23687
VAR51	eto-minf	-0.11508	0.22580	0.01577	0.11162	0.08666
VAR52	eto-minw	-0.10114	0.21505	-0.00797	0.00996	-0.07724
VAR53	eto-maxsp	-0.11319	0.30377	0.03476	0.14958	0.05143
VAR54	eto-maxsu	-0.12194	0.17147	0.06266	0.22705	0.19068
VAR55	eto-maxf	-0.08000	0.25199	-0.03264	0.20395	-0.07998
VAR56	eto-maxw	-0.09242	0.24250	0.01213	0.00977	-0.08323
VAR57	eto-avgsp	-0.11526	0.23413	0.04426	0.14934	0.04450
VAR58	eto-avgsu	-0.13722	0.17167	-0.01058	0.27614	0.22394
VAR59	eto-avgf	-0.10516	0.24775	-0.00915	0.16213	-0.01096
VAR60	eto-avgw	-0.07662	0.22288	0.00303	-0.05244	-0.09554
			GDD			
VAR61	gddsp	0.11312	0.00599	-0.03034	0.13090	0.21253
VAR62	gddsu	0.17077	-0.01446	-0.01383	0.10592	0.08954
VAR63	gddf	0.15094	0.01208	-0.06947	0.08581	0.09602
VAR64	gddw	0.07279	0.07002	0.09964	-0.12650	0.09951
			Frosty days			
VAR65	frz_free	0.11368	0.11417	-0.14843	-0.09487	-0.09497
VAR66	frz_fall	0.13310	0.10408	-0.09587	-0.12554	-0.08497
VAR67	frz_spr	-0.13050	-0.11077	0.12722	0.01679	0.04943

* t; temperature, ppt; precipitation, eto; reference evapotranspiration, min; minimum, max; maximum, avg; average, sp; spring, su; summer, f; fall, w; winter, gdd; growth degree days, frz-free; frostless days, frz-fall; fall frost days, frz-spr; spring frost days.